Journal of Molecular Graphics and Modelling 29 (2011) 693–701

Contents lists available at ScienceDirect

Journal of Molecular Graphics and Modelling

journal homepage: www.elsevier.com/locate/JMGM

Computational investigation of interactions between human H_2 receptor and its agonists

Xianqiang Sun, Yaozong Li, Weihua Li, Zhejun Xu, Yun Tang*

Department of Pharmaceutical Sciences, School of Pharmacy, East China University of Science and Technology, 130 Meilong Road, Shanghai 200237, China

ARTICLE INFO

Article history:
Received 19 August 2010
Received in revised form
23 November 2010
Accepted 4 December 2010
Available online 13 December 2010

Keywords:
Histamine receptors
H_2R agonists
Pharmacophore modeling
Homology modeling
Molecular docking

ABSTRACT

Type 2 histamine receptor (H_2R) is widely distributed in the body. Its main function is modulating the secretion of gastric acid. Most gastric acid-related diseases are closely associated with it. In this study, a combination of pharmacophore modeling, homology modeling, molecular docking and molecular dynamics methods were performed on human H_2R and its agonists to investigate interaction details between them. At first, a pharmacophore model of H_2R agonists was developed, which was then validated by QSAR and database searching. Afterwards, a model of the H_2R was built utilizing homology modeling method. Then, a reference agonist was docked into the receptor model by induced fit docking. The 'induced' model can dramatically improve the recovery ratio from 46.8% to 69.5% among top 10% of the ranked database in the simulated virtual screening. The pharmacophore model and the receptor model matched very well each other, which provided valuable information for future studies. Asp98, Asp186 and Tyr190 played key roles in the binding of H_2R agonists, and direct interactions were observed between the three residues and agonists. Residue Tyr250 could also form a hydrogen bond with H_2R agonists. These findings would be very useful for the discovery of novel and potent H_2R agonists.

1. Introduction

Histamine is a neurotransmitter and plays many roles in human body. To date, four histamine receptor subtypes have been identified [1]. Among them, type 2 histamine receptor (H_2R) is widely distributed and functions as a modulator in gastric acid secretion. Dysfunction of H_2R may cause peptic ulcer or other gastric acid-related diseases [2]. H_2R also plays some other important roles. For example, in heart, the receptor performs as a mediator in the chronotropic response to histamine; while in lung, it acts as a modulator. It also plays an unidentified role in brain [3]. Thus, H_2R is an attractive drug target.

H_2R belongs to the superfamily of G-protein coupled receptors (GPCRs). However, its three-dimensional structure has not been determined yet. To date, many H_2R ligands have been discovered for clinic usages. H_2R antagonists Cimetidine and Ranitidine are widely used in clinic for the treatment of peptic ulcers. Nevertheless, H_2R agonists can also be developed to treat heart failure [4], acute myelogenous leukemia [5], or as anti-inflammatory agents [6], but no H_2 agonists are used in clinic yet.

Impromidine was the first H_2R agonist discovered by Durant et al. in 1978. It was >50 times potent than histamine at the guinea pig right atrium and was investigated for the treatment of catecholamine-insensitive congestive heart failure [7]. Arpromidine was another H_2R agonist with high potency synthesized by Buschauer in 1989 [8]. An increasing number of potent impromidine-like and histamine-like agonists were reported in recent years [8–14].

H_2R agonists can be divided into two subsets: amine-type and guanidine-type. Computer-aided methods, such as 3D-QSAR analysis, have been used to study the guanidine-type agonists and valuable information was obtained [15,16]. It was confirmed that branching at the third C atom after the guanidino group could increase the activity of the agonists [9,10]. However, it is difficult for the 3D-QSAR analysis to provide information to find ligands with novel scaffolds. Pharmacophore modeling is another widely used ligand-based method for drug discovery. It can be used to discover novel ligands with diverse chemical types [17–19]. Many pharmacophore models have been built for GPCR ligands [20,21], but none was reported for H_2R agonists.

Similar to other GPCRs, H_2R receptor consists of seven transmembrane helices (TH1–TH7), three extracellular (ECL1–ECL3) and three intracellular (ICL1–ICL3) loops [2]. Previous mutation studies on the receptor demonstrated that residues Asp98, Asp186 and Thr190 were essential for the binding of histamine [22,23], which was consistent with the three-site model proposed by Weinstein et al. [24]. Meanwhile, H_2R models were constructed to explain the ligand–receptor interactions. These models were valuable for

* Corresponding author. Tel.: +86 21 64251052; fax: +86 21 64253651.
E-mail address: ytang234@ecust.edu.cn (Y. Tang).

1093-3263/$ – see front matter © 2010 Elsevier Inc. All rights reserved.
doi:10.1016/j.jmgm.2010.12.001

rational ligand design [9,10,23]. Nevertheless, the binding modes of agonists were not quite consistent with the experimental studies [23], and manual docking of ligands might introduce biases or errors [9,10]. Recent years witness great progresses in the crystallization of GPCRs [25–27], which would surely facilitate the homology modeling of H_2R. Precise docking methods then could be used to study the binding modes of H_2R agonists with the receptor.

In this work, pharmacophore models for H_2R agonists were generated at first. A homology model of human H_2R was also constructed based on the crystal structure of β_1-adrenoceptor [26]. Detailed interactions between agonists and the receptor were then elucidated. A protocol combining ligand-based and receptor-based methods together was established to facilitate the development of novel and selective H_2R agonists.

2. Materials and methods

2.1. Pharmacophore modeling

Phase, embedded in the Schrödinger software package, was applied to generate the pharmacophore models [28].

2.1.1. Compound preparation

Totally 62 H_2R agonists were collected from publications, whose bioactivities were determined by the same group [9–12,29,30]. Compounds with $EC_{50} \leq 50$ nM were regarded as active ones; whereas those with $EC_{50} \geq 1000$ nM were treated as inactive ones (Table 1). The remaining molecules were used to validate the pharmacophore models (SI. 1).

The chemical structures of the compounds were sketched with ISIS/Draw and imported into Phase [28], where LigPrep [31] was called to generate reasonable 3D neutralized structures. Then, a combination of Monte-Carlo Multiple Minimum sampling and Low Mode conformational searching was introduced to generate the conformers [32] of each molecule. A maximum of 1000 conformers, OPLS-2005 force field, implicit GB/SA solvent model, a relative conformational energy of 10 kJ/mol, and a redundancy check of 2 Å in the heavy atom positions were set in the conformer generation procedure.

2.1.2. Pharmacophore generation

Default pharmacophore feature definitions, i.e. hydrogen bond acceptor (HA), hydrogen bond donor (HD), hydrophobic (HY), positive charged group (PI), ring aromatic (AR), and negatively charged group (N), were used in pharmacophore generation. The minimum and maximum numbers of the features in a particular pharmacophore model were set as four and five, respectively. According to the structural properties of the agonists, one HD and one PI were specified in pharmacophore generation. The processes of scoring with respect to the actives were conducted using default parameters. Hypotheses that emerged from this process were subsequently scored with the inactive compounds, with the weight of 1.

2.1.3. Pharmacophore validation with QSAR

Phase offers two methods to built QSAR models. One is atom-based method, and the other is pharmacophore-based method. In this study, the atom-based 3D-QSAR models were developed based on the alignments by pharmacophore. Half of the 62 ligands were selected as the training set in accordance with the usual guidelines, and the others were used as the test set. Since the maximum number of the partial least squares (PLS) factor should be smaller than 1/5 of the number of the training set molecules, PLS regressions were performed with the PLS factors 1–5.

2.1.4. Enrichment factor from pharmacophore searching

Enrichment factor (EF_P) could indicate the capability of a pharmacophore in identifying active compounds. The optimal pharmacophore was used to screen a molecular database to get the EF_P. The database was established by the following procedure. At first, three compound databases, namely Maybridge, NCI and Specs, were downloaded from the ZINC database [33]. All the databases were merged together, which led to a large database containing 694,292 small molecules. FCFP_4 fingerprint in Discovery Studio 2.1 was employed to concentrate the merged database into a structurally diverse one, including 50,000 chemicals. Then, 49 known H_2R agonists, which were not used in the pharmacophore generation, were seeded into the diverse database. Finally, 38 other subtype selective ligands, i.e. one H_1 selective agonist, 12 H_1 selective antagonists, seven H_2 selective antagonists, 13 H_3 and H_4 selective agonists, and five H_3 and H_4 selective antagonists, were put into the database to test the selectivity of the model (see SI.2 for detailed structures of the 38 ligands). ConfGen with default parameters was used to generate the conformers for the small molecules in the database. EF_P was calculated utilizing the following equation [34].

$$EF_P = \left(\frac{H_a}{H_t}\right) / \left(\frac{A}{D}\right)$$

H_t represents the number of hits retrieved, H_a represents the number of active molecules in the hit list, A represents the number of active molecules presenting in the database, and D is the total number of molecules in the decoy database.

2.2. Homology modeling

Homology modeling was conducted with the Prime program of Schrödinger software package [35].

2.2.1. Sequence alignment and model construction

The primary sequence of human H_2R receptor was retrieved from the Protein Information Resource [36]. The crystal structure of the β_1-adrenoceptor [26] (PDB entry 2vt4) was used as the template (approximately 38% sequence identity). Automatic sequence alignment was employed by ClustalW2 [37] to make sure that the conserved GPCR elements were placed in the right position. The alignment was then manually modified to make sure that there were no gaps in the second structures and the conserved (Cys-Cys) disulfide bridges were maintained. The loop ICL3 was constructed with Prime automatically.

2.2.2. Docking the reference molecule into the model

Induced Fit Docking (IFD) protocol in Schrödinger software package [38] was used to dock the reference agonist to the receptor model. This protocol is capable of sampling not only dramatic side chain conformational changes by Prime on residues within 5 Å of the ligand pose, but also minor changes in the backbone produced by Prime minimization on the same set of residues (i.e. flexible ligand and flexible target). Default parameters were used in this procedure. Compound **5** was selected as the reference compound. Asp98 and Asp186 were reported as important residues in the binding of agonists [22] and hence picked as the center of the grid. Finally, 20 complex structures were obtained. One of them, which was consistent with reported mutation data [22,23], was chosen for the following studies.

2.2.3. Molecular dynamics simulation of receptor–agonist complex

In order to explore the detailed interactions between the receptor and its agonist, molecular dynamics (MD) simulation was

Table 1
Structures and EC_{50} of the compounds in the active set and inactive set.

No.	Structure	EC_{50} (nM)	No.	Structure	EC_{50} (nM)
1	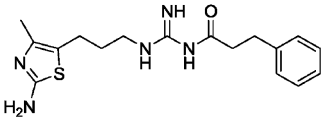	22.2	**2** *	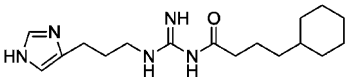	23
3*	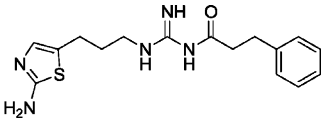	23.8	**4***	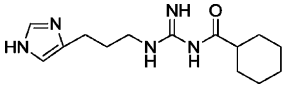	38
5*	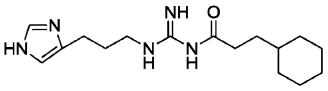	46	**6**	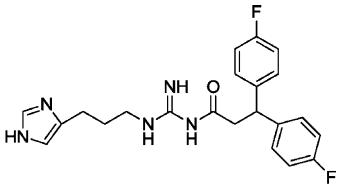	48
7	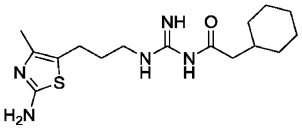	49.7	**8***	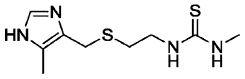	1400
9*	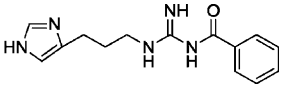	1400	**10**	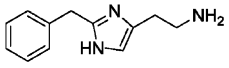	13,000
11*	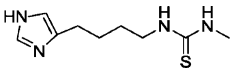	14,000	**12**	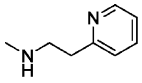	44,000

* Training set molecules that were applied to QSAR generation.

performed on the IFD-generated complex model with the program Desmond [39,40] and OPLS-AA force field [41]. POPC [42] membrane system and TIP3P [43] water model were used in the simulation.

The membrane was placed using the information provided by the OPM database [44–46], where the membrane information of β_1-adrenoceptor was included. The membrane information of β_1-adrenoceptor was then copied to the H_2 receptor through dummy atoms.

The cubic box was generated with Maestro, keeping any atoms of the solute at least 10 Å away from each edge of the box. 13 chloride ions were added to neutralize the system. Salt concentration of the system was set to 0.15 M Na^+/Cl^-. A 12 Å cut-off value was used for the nonbonded interactions. The simulations were performed with periodic boundary conditions. Before MD simulation, energy minimizations were carried out with steepest decent algorithm, followed by conjugate gradient one. The detailed minimization protocol was described in Table 2. Simulations utilized NPT ensembles with the Martyna–Tobias–Klein pressure coupling and the Nose–Hoover temperature coupling with default parameters. The time-steps of bonded interactions and near non-bonded interactions were set as 1 fs, far non-bonded interaction time-step was set as 3 fs [39]. All constraints were implemented by the M-SHAKE algorithm [47]. The simulation was performed for 1.2 ns.

Table 2
Minimization protocol of the human H_2R-compound **5** system.

Procedure	Steps	Human H_4R–agonist complex	TIP3P	POPC
1	20,000	Freezing	Move	Freezing
2	20,000	Freezing	Move	Move
3	20,000	Move	Move	Move

2.2.4. Model validation with virtual screening

Virtual screening was carried out to assess the receptor model. The database contained 47 H_2 agonists, 38 other subtype selective ligands and 620 assumed inactive compounds. LigPrep [31] was called to generate all the possible protonation states for these compounds at pH 5–9. Three H_2 receptor models, including the initial model, the model after IFD (the 'induced' model) and the one after MD simulation (the 'MD' model), were used in this procedure.

Glide with standard precision (SP) was used in the simulated virtual screening. Asp98 and Asp186 were also used to define the centre of the grid. The best docking pose of each compound was chosen with GlideScore. Enrichment factors of the docking (EF_D) were calculated in a similar way with EF_P.

2.2.5. Energy contribution of Tyr250 in agonist binding

Glide docking could detect per-residue interactions between the ligand and the receptor. Tyr250 was supposed to be important in this study. Therefore, the energy contribution of Tyr250 was detected utilizing Glide docking. To do this, all the 62 active compounds mentioned above were docked to the 'induced' H_2 model. Then the energy contribution of Tyr250 was analyzed.

3. Results

3.1. H_2 agonist pharmacophore

3.1.1. Optimal pharmacophore selection

Totally 231 pharmacophore models were generated (SI. 3). The best pharmacophore was selected based on previous studies [15,16,22,23] and the following QSAR indicators. As illustrated in Fig. 1A, the best pharmacophore model included four features:

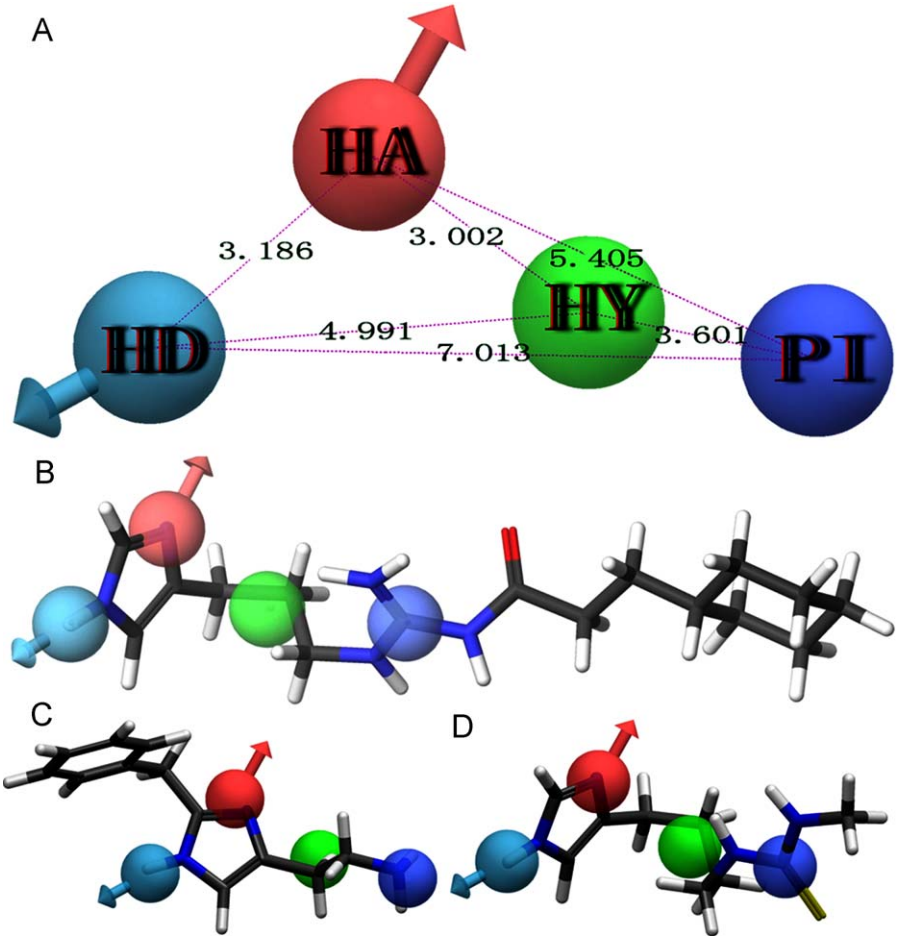

Fig. 1. The best pharmacophore model produced by Phase. (A) Schematic representation of the pharmacohore; (B) reference compound 5 mapping to the pharmacophore; (C) compound **10** mapping to the pharmacophore; (D) compound **11** mapping to the pharmacophore. Pharmacophore features are color-coded: *red* hydrogen bond acceptor (HA), *light blue* hydrogen bond donor (HD), *dark blue* positive charged group (PI), *green* hydrophobic (HY). The unit of all the distances is in Angstrom (Å). The 3D images were created using Maestro. (For interpretation of the references to color in this figure legend, the reader is referred to the web version of the article.)

one HA, one HD, one PI and one HY. Compound **5** was automatically selected as the reference molecule. Fig. 1B–D showed how compounds **5**, **10** and **11** matched to the pharmacophore model, respectively. From Fig. 1B, it is obvious to see that the imidazolylpropylguanidine moiety of compound **5** contains all the four features, so it should be the key for the agonistic activity of the compound. Compound **10** belongs to the amine-type agonists and a stereo-specific blockade to the agonist binding is noticed, which might be the reason of losing activity (Fig. 1C). PI is a very important feature according to the mutation studies [22]. However, compound **11** missed this feature (Fig. 1D), which might explain why the compound lost activity.

3.1.2. QSAR activity prediction

The selected 62 human H_2R agonists, whose bioactivities were measured by Buschauer and his coworkers, were used to build the QSAR models. From the superposition of the agonists with the pharmacophore, there were no pharmacophore features mapping to the chiral centre in alkyl side chains, so the chirality of the compounds were ignored. The chirality was also neglected in pervious 3D-QSAR study on the H_2 agonists [15,16], and experiments also demonstrated that α or β position chirality played minor role in H_2 activation [48]. When PLS factor was set as 3, the best QSAR model was obtained with $R^2 = 0.90$ for the training set and $Q^2 = 0.66$ for the test set (Fig. 2).

3.1.3. Enrichment factor of pharmacophore

Among the 49 H_2R agonists seeded in the database, the pharmacophore model retrieved 47 ones. 11 out of the 38 ligands with other subtype selectivity and 620 decoys were also obtained with the model. Therefore, the enrichment factor EF_P was 70.02 at this

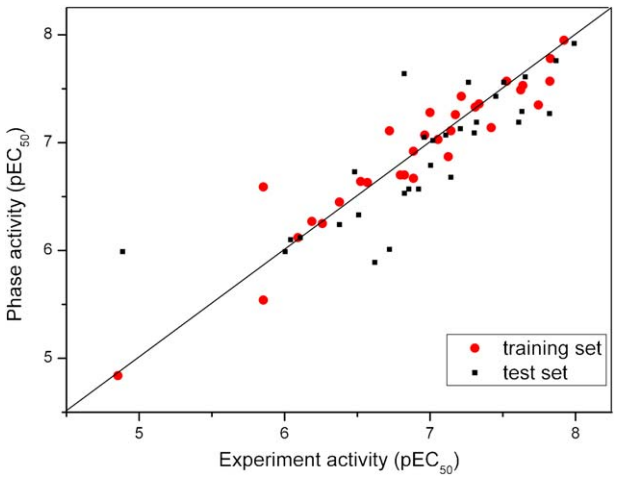

Fig. 2. Scatter plots of predicted and experimental pEC50 of human H_2R agonists. The R^2 gets the value of 0.90 and Q^2 is 0.66.

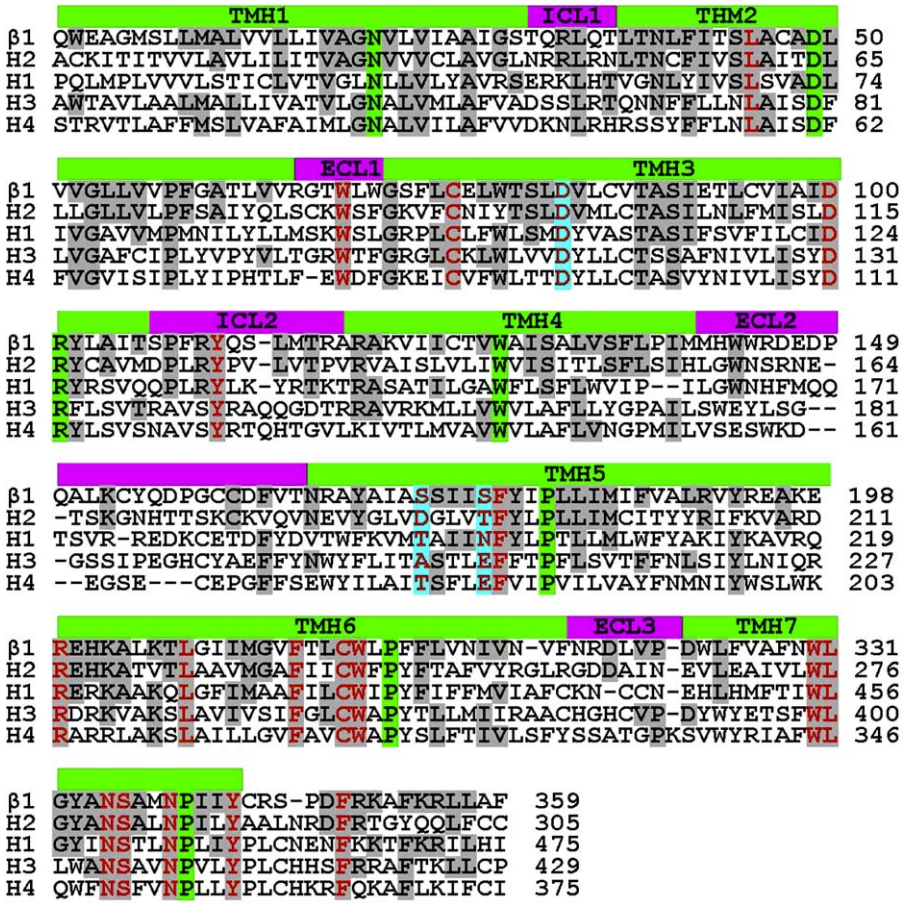

Fig. 3. Alignment of the human H_1, H_2, H_3 and H_4 receptor sequences with β1-adrenoceptor. Highly conserved residues are highlighted in red. The key residues involved in agonists or antagonists binding are highlighted in cyan. The identical residues between the histamine receptors and the β1-adrenoceptor are colored with the gray background. (For interpretation of the references to color in this figure legend, the reader is referred to the web version of the article.)

stage, which meant that the pharmacophore was good enough to identify H_2R selective agonists from many others.

3.2. Homology modeling of the receptor

3.2.1. Model generation

Sequence alignments among β_1-adrenoceptor and human H_2 as well as H_1, H_3 and H_4 receptors were shown in Fig. 3. The sequence identities between the four histamine receptors and β_1-adrenoceptor were 34%, 38%, 28%, and 21%, respectively. The ultimate alignment was highly consistent with the published works [49].

ICL3 has no equivalent region in the crystal structure of β_1-adrenoceptor, and it does not contribute to the ligand binding. Therefore, the ICL3 was modeled automatically, and then minimized by 5000 iterations with MacroModel [50]. From Ramachandran plot of the model [51], we can see that 93.4% of the residues are in the most favored regions, 5.8% in the allowed regions, and only one residue in the disallowed regions (SI. 4). The RMSD between the model and its template was only 0.53 Å.

3.2.2. Docking of the reference ligand

Published papers indicated that histamine bound to the receptor as a monocation in its proximal tautomeric form [52–54]. Likewise, compound **5** was docked to the homology model in the same protonation state as histamine. 20 complexes were obtained and the optimal complex was selected based on the contacts observed between the ligand and the receptor. Available mutation results also supported the docking model [22,23], for example, residues Asp98, Asp186 and Thr190 were identified as key residues [22].

Fig. 4 illustrated the optimal receptor–agonist complex after minimization, taking the pharmacophore as a reference. The picture clearly showed that the four pharmacophore features matched well with the receptor. The PI feature matched with the negatively charged residue Asp98. The HA feature was mapped to atom N^{τ} in the imidazole ring. A hydrogen bond formed between atom N^{τ} and the carboxylate oxygen of Asp186. Atom N^{π} in the imidazole ring acted as a hydrogen bond acceptor and a hydrogen bond formed with Thr190. The HY centre coincided with the hydrophobic interactions between the imidazolylpropyl side chain and the receptor. The hydrophobic pocket consisted of residues Phe251, Try250, Trp247, Val99, and Cys102. The RMSD between the two poses was 4.1 Å. If the alkyl chain branching was not considered, the RMSD was only 1.63 Å. The imidazolylpropylguanidine moiety of compound **5** bound to the receptor in a similar way as histamine [55]. AS for the other H_2R agonists in the training set and test set, the RMSDs between the docking pose and the pharmacophore pose were also obviously bigger when the alkyl chain branching were included. This could be demonstrated by the cumulative percentage curve in Fig. 5.

3.2.3. MD simulation of receptor–agonist complex

MD simulation was performed with the complex embedded in the membrane (the model was deposited as SI. 5). The RMSD of the α-carbon atoms demonstrated that the simulation was equilibrated after 0.6 ns (Fig. 6). The key interactions between compound

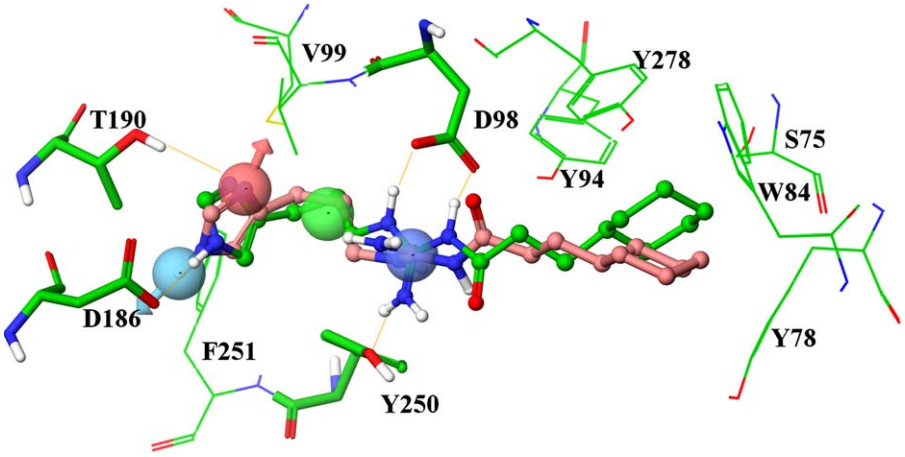

Fig. 4. Detail of human H_2R-compound **5** complex matched with the pharmacophore. Human H_2R-compound 5 complex is colored with green carbon; the pharmacophore conformation of compound **5** is colored in pink. The 3D images were created using Maestro. (For interpretation of the references to color in this figure legend, the reader is referred to the web version of the article.)

5 and the receptor maintained well during the simulation. The ionic interaction between the guanidinium group and Asp98 presented during the whole simulation. The distance between the carboxylate carbon of Asp98 and the positive charge centre of the guanidinium group fluctuated between 3.56 Å and 4.04 Å, and the average distance was 3.81 Å (Fig. 6A). The hydrogen bond between Asp186 and the imidazole ring N^{τ} was maintained during the simulation, and the distance fluctuated between 1.48 Å and 3.15 Å (Fig. 6C). Thr190 hydroxyl hydrogen directed to imidazole ring N^{π} during 0–0.2 ns and 0.6–0.95 ns to form a hydrogen bond interaction (Fig. 6D).

MD simulation also demonstrated the role of Try250 in agonists binding. A hydrogen bond was observed between the guanidine hydrogen and the Try250 carboxylate oxygen almost in the whole simulation, and the distance fluctuated between 1.63 Å and 2.76 Å (Fig. 6B).

3.2.4. Receptor model validation by virtual screening

The 678 compounds retrieved by the pharmacophore and all the ligands with subtype selectivity were combined to constitute a focused database. Based on this database, Glide SP docking was employed to run a simulated virtual screening with the initial receptor model, the 'induced' model, and the 'MD' model.

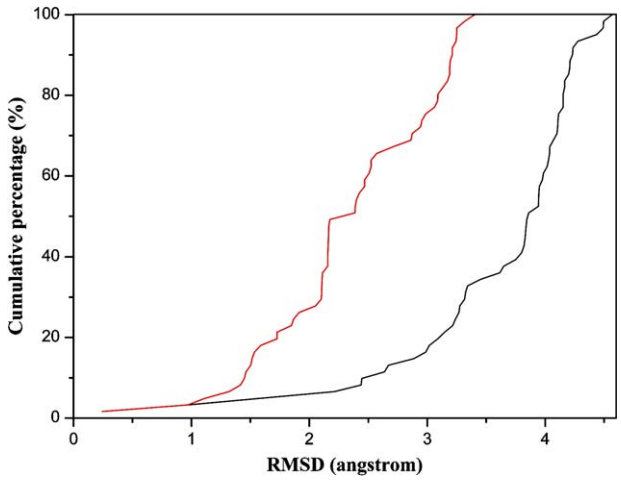

Fig. 5. Cumulative percentage curve about the RMSD of the agonists between the pharmacophore poses and the docking poses. The RMSD cumulative percentage curve without considering the branching is represented with the red line; the black line represents the RMSD cumulative percentage curve when the branching is included. (For interpretation of the references to color in this figure legend, the reader is referred to the web version of the article.)

The docking results were presented as enrichment curves in Fig. 7. The initial model could retrieve 5, 9, and 21 H_2R agonists with respect to 2%, 5% and 10% of the ranked database, and the $EF_D^{X\%}$ values were 5.85, 4.28 and 4.99, respectively. The 'MD' model performed much better than the initial model with the corresponding values of $EF_D^{X\%}$ as 6.43, 8.15 and 6.60. Moreover, the 'induced' model performed best among the three models, and the corresponding values of $EF_D^{X\%}$ were 11.9, 9.12 and 6.95, respectively.

The compounds retrieved by pharmacophore searching were also ranked by the fitness values to get the enrichment curve. As assumed, the enrichment curve of the pharmacophore was worse than those of the three receptor models. Therefore, although the pharmacophore could concentrate the database, its capability in selecting active compounds was weak. To analyse the retrieving ability of the models, the area under the curve (AUC) was also calculated for the three enrichment curves in Fig. 7, and the results were listed in Table 3. The 'induced' model and the 'MD' model got the highest AUC value of 0.87, which meant these two models possessed the best property in recovering active compounds.

Ligands with different subtype selectivities were seeded in the database and used as an indicator of the models. At 10% of the ranked database, the initial model retrieved 5 ligands with other subtype selectivity, and the 'MD' model retrieved 1. The 'induced' model performed best and retrieved none. This meant that the 'induced' model possesses a strong ability in ranking H_2R agonists to top 10% of the database.

3.2.5. Energy contribution of Tyr250 in virtual screening

Since Tyr250 was recognized as an important residue to H_2 agonist binding during the MD simulation, the energy contribution of Tyr250 in the binding of H_2 agonists was calculated based on the 'induced' model, and the detailed information was listed

Table 3
AUC of the enrichment plots for the pharmacophore model, the initial model, the 'MD' model and the 'induced' model.

Model	AUC
Phamacophore model	0.70
Initial model	0.71
MD model	0.87
Induced model	0.87

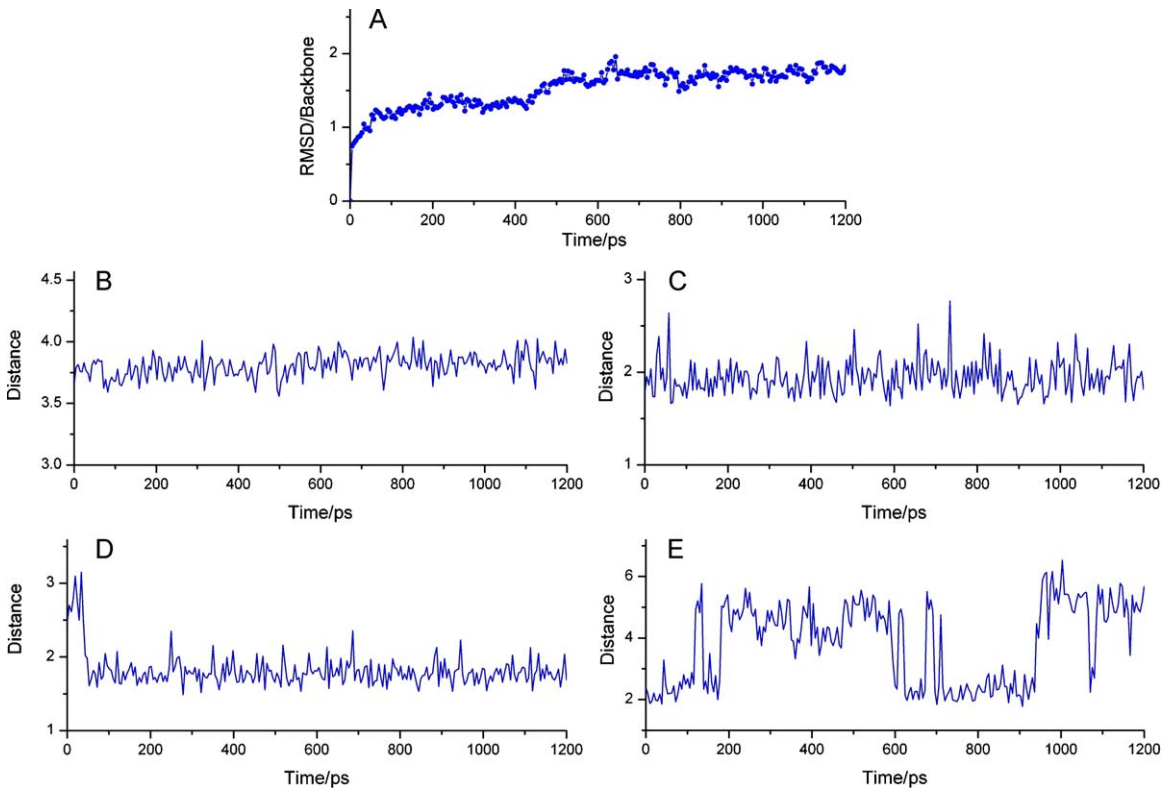

Fig. 6. The result about the MD simulation. The unit of all the distances is in Angstrom (Å). (A) The RMSD of the α-carbon in the simulation. (B) The distance fluctuation between the carboxylate carbon of Asp98 and the positive charge centre of the guanidinium group. (C) The distance fluctuation between carboxylate oxygen of Tyr250 and the closest hydrogen in the guanidinium group. (D) The distance fluctuation between the imidazole ring N^{τ} and the carboxylate oxygen of Asp186. (E) The distance fluctuation between the imidazole ring N^{π} and the Thr190 hydroxyl hydrogen.

in SI. 6. For most H_2 agonists, Tyr250 played a positive role in the binding, and the average energy contribution of Tyr250 was −6.21 kcal/mol.

4. Discussion

Computer-aided drug design (CADD) has been used in almost every stage of drug research and development, which changes the strategy and pipeline of drug discovery greatly [56]. In this study, a variety of CADD methods were employed, and useful information was obtained from both ligand and receptor sides.

4.1. Coincidence of pharmacophore model with homology model

The pharmacophore model was compared with the receptor model carefully. All the pharmacophore features had a corresponding region in the receptor model (Fig. 1A). The PI feature, corresponding to the guanidinium group of compound **5**, formed an electrostatic interaction with the negatively charged carboxyl group of Asp98. The HD and HA features matched the imidazole ring of compound **5**, and formed hydrogen bonds with residues Asp186 and Thr190. Hydrophobic interactions could increase the binding affinity. Hence, the HY feature was also important in our pharmacophore model.

The computational studies were also consistent with previous mutation experiments [22,23]. Previous studies demonstrated that H_2 receptor was activated by a proton transfer between a hydrogen bond donor and acceptor [52]. This tautomerisation might happen by the couples Tyr182/Asp186 [53] or Asp186/Thr190

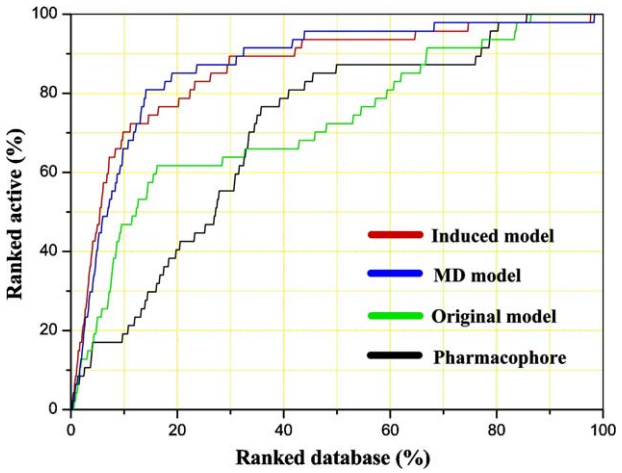

Fig. 7. Enrichment plots for human H_2R models and the pharmacophore.

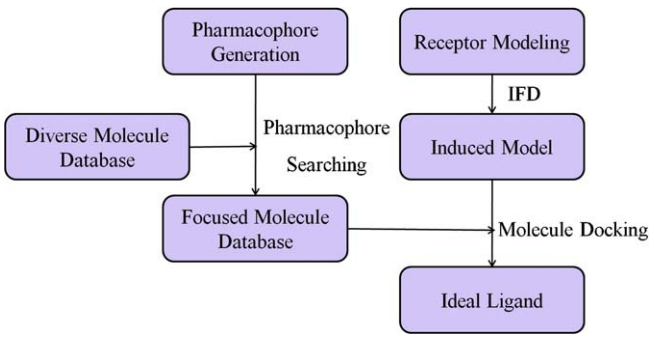

Fig. 8. Protocol of discovering novel ligands for the GPCRs.

[22] Tyr182 or Thr190 would act as a proton donor and Asp186 as a proton acceptor. Previous homology models preferred to the Tyr182/Asp186 binding mode [23,53]. However, site-directed mutagenesis studies demonstrated that mutations Asp186Ala and Thr190Ala dramatically decreased the efficacy of histamine alone or simultaneously [22]. Therefore, our Asp186/Thr190 activation model (Fig. 4) was reasonable.

From our study, a hydrogen bond was formed between Tyr250 and the guanidinium group of the agonist in the receptor–ligand complex (Fig. 4). Thus, we proposed that Tyr250 might play an important role in agonist binding.

4.2. Information from MD simulation

MD simulation was performed on the receptor–compound **5** complex. Although the time length was only 1.2 ns, some useful information could be obtained. During the simulation, the interactions between the ligand and the receptor kept stable except for a waggling of the hydrogen bond between the Tyr190 and N^{π} in the imidazole ring (Fig. 6). Obviously, this wagging can stabilize the tautomer after the transport of $O\cdots H \rightarrow N^{\pi}$, because the deflection of Thr190 side chain oxygen can reduce the constraint on the transferred proton in the N^{π}. This is also consistent with previous mutation studies by Gantz et al., which showed that amino acid residue in the TH5 (Thr190) was important in establishing the kinetics of histamine binding and action, but not an essential component of H_2R selectivity [22].

The hydrogen bond between the guanidinium group and the side chain oxygen of Tyr250 was maintained during the whole simulation. Thus, we can infer the importance of Tyr250 in fixing the agonists to the receptor from the available data.

4.3. Implications for the discovery of novel and selective H_2 agonists

Combining ligand-based and receptor-based methods together in drug design has been widely used [57]. When virtual screening was utilized to find new hits, pharmacophore searching could be used to screen databases in seconds. However, the enrichment curve of pharmacophore searching was obviously lower than that from the structural model (Fig. 7). Conversely, Glide docking can enrich most of the active molecules in top 10% of the database, but it is time consuming. Therefore, we can combine our validated pharmacophore model and the receptor model together to discover new H_2 agonists.

To do so, the following procedures are suggested. At first, pharmacophore searching is performed to screen a diverse database. Most of the inactive compounds could be removed in this procedure. Then, the molecules matched with the pharmacophore are docked into the binding pocket of the receptor. Afterwards, the promising molecules can be selected for bioassay according to docking score and visual analysis. In the case of X-ray crystal structure of the receptor unavailable, homology models can be used for molecular docking. Then, the IFD can be utilized to reshape the binding pocket of the receptor. The whole procedure of this protocol is displayed in Fig. 8. This protocol could be helpful for ligand discovery of GPCRs.

Ligand selectivity is still a tough issue, especially for GPCRs. In our case, all the models possessed strong capabilities in identifying H_2R agonists. Especially, the 'induced' model performed best both on the $EF_D^{X\%}$ and selectivity (Fig. 7). Therefore, our 'induced' model possesses a specific binding pocket for the H_2 agonists, and it could be used for the discovery of novel selective H_2 agonists.

From our virtual screening, some diverse molecules were found. As shown in the supporting information (SI. 7), these molecules not only matched the pharmacophore features very well, but also formed reasonable interactions with key residues in the receptor. Bioassays are necessary to confirm if these molecules are selective H_2 agonists.

5. Conclusions

In summary, we have systematically studied human H_2R and agonists by various methods, including pharmacophore modeling, homolog modeling, molecule docking, and molecular dynamic simulation. All the data were cross validated with each other. The pharmacophore model and the homology model were in good agreement. The HA/Tyr190, HD/Asp186 and PI/Asp98 three matching pairs formed on the view of both ligands and receptor. Residue Tyr250 was found very important to the binding of H_2R agonists. These two models can be combined together to facilitate the discovery of novel and selective human H_2 agonists.

Acknowledgements

This work was supported by the Program for New Century Excellent Talents in University (Grant NCET-08-0774), the 863 High-Tech Project (Grant 2006AA020404), the 111 Project (Grant B07023), and the National S&T Major Project of China (Grant No. 2009ZX09501-001).

Appendix A. Supplementary data

Supplementary data associated with this article can be found, in the online version, at doi:10.1016/j.jmgm.2010.12.001.

References

[1] M. Jutel, M. Akdis, C.A. Akdis, Histamine, histamine receptors and their role in immune pathology, Clinical and Experimental Allergy 39 (2009) 1786–1800.
[2] S.J. Hill, C.R. Ganellin, H. Timmerman, J.C. Schwartz, N.P. Shankley, J.M. Young, W. Schunack, R. Levi, H.L. Haas, International Union of Pharmacology. XIII. Classification of histamine receptors, Pharmacol. Rev. 49 (1997) 253–278.
[3] M.E. Parsons, C.R. Ganellin, Histamine and its receptors, Br. J. Pharmacol. 147 (Suppl. 1) (2006) S127–135.
[4] J. Kim, A. Gai, S. Nakatani, K. Hashimura, H. Kanzaki, K. Komamura, M. Asakura, H. Asanuma, S. Kitamura, H. Tomoike, M. Kitakaze, Impact of blockade of histamine H-2 receptors on chronic heart failure revealed by retrospective and prospective randomized studies, J. Am. Coll. Cardiol. 48 (2006) 1378–1384.
[5] R. Seifert, A. Hoer, I. Schwaner, A. Buschauer, Histamine increases cytosolic Ca2+ in HL-60 promyelocytes predominantly via H2 receptors with an unique agonist/antagonist profile and induces functional differentiation, Mol. Pharmacol. 42 (1992) 235–241.
[6] R. Burde, A. Buschauer, R. Seifert, Characterization of histamine H2-receptors in human neutrophils with a series of guanidine analogues of impromidine. Are cell type-specific H2-receptors involved in the regulation of NADPH oxidase? Naunyn Schmiedebergs Arch. Pharmacol. 341 (1990) 455–461.
[7] G.J. Durant, W.A. Duncan, C.R. Ganellin, M.E. Parsons, R.C. Blakemore, A.C. Rasmussen, Impromidine (SK&F 92676) is a very potent and specific agonist for histamine H2 receptors, Nature 276 (1978) 403–405.
[8] A. Buschauer, Synthesis and in vitro pharmacology of arpromidine and related phenyl(pyridylalkyl)guanidines, a potential new class of positive inotropic drugs, J. Med. Chem. 32 (1989) 1963–1970.
[9] A. Kraus, P. Ghorai, T. Birnkammer, D. Schnell, S. Elz, R. Seifert, S. Dove, G. Bernhardt, A. Buschauer, N(G)-acylated aminothiazolylpropylguanidines as potent and selective histamine H(2) receptor agonists, ChemMedChem. 4 (2009) 232–240.
[10] P. Ghorai, A. Kraus, M. Keller, C. Gotte, P. Igel, E. Schneider, D. Schnell, G. Bernhardt, S. Dove, M. Zabel, S. Elz, R. Seifert, A. Buschauer, Acylguanidines as bioisosteres of guanidines: NG-acylated imidazolylpropylguanidines, a new class of histamine H2 receptor agonists, J. Med. Chem. 51 (2008) 7193–7204.
[11] S.X. Xie, A. Kraus, P. Ghorai, Q.Z. Ye, S. Elz, A. Buschauer, R. Seifert, N1-(3-cyclohexylbutanoyl)-N2-[3-(1H-imidazol-4-yl)propyl]guanidine (UR-AK57), a potent partial agonist for the human histamine H1- and H2-receptors, J. Pharmacol. Exp. Ther. 317 (2006) 1262–1268.
[12] M.T. Kelley, T. Burckstummer, K. Wenzel-Seifert, S. Dove, A. Buschauer, R. Seifert, Distinct interaction of human and guinea pig histamine H2-receptor with guanidine-type agonists, Mol. Pharmacol. 60 (2001) 1210–1225.
[13] J. Christiaans, H.v.d. Goot, W. Menge, H. Timmerman, Synthesis and in vitro pharmacology of dimaprit analogues with histamine Hz-agonistic and HI-antagonistic activities, Eur. J. Med. Chem. 30 (1995) 673–678.

[14] J.C. Eriks, H. van der Goot, G.J. Sterk, H. Timmerman, Histamine H2-receptor agonists. Synthesis, in vitro pharmacology, and qualitative structure-activity relationships of substituted 4- and 5-(2-aminoethyl)thiazoles, J. Med. Chem. 35 (1992) 3239–3246.
[15] S. Dove, A. Buschauer, Imidazolylpropylguanidines as histamine H2 receptor agonists: 3D-QSAR of a large series, Pharm. Acta Helv. 73 (1998) 145–155.
[16] S. Dove, A. Buschauer, Improved alignment by weighted field fit in CoMFA of histamine H-2 receptor agonists imidazolylpropylguanidines, Quant. Struct.-Act. Rel. 18 (1999) 329–341.
[17] J. Zou, H.Z. Xie, S.Y. Yang, J.J. Chen, J.X. Ren, Y.Q. Wei, Towards more accurate pharmacophore modeling: multicomplex-based comprehensive pharmacophore map and most-frequent-feature pharmacophore model of CDK2, J. Mol. Graph. Model. 27 (2008) 430–438.
[18] F. Cheng, Z. Xu, G. Liu, Y. Tang, Insights into binding modes of adenosine A2B antagonists with ligand-based and receptor-based methods, Eur. J. Med. Chem. 45 (2010) 3459–3471.
[19] S.Y. Yang, Pharmacophore modeling and applications in drug discovery: challenges and recent advances, Drug Discov. Today. 15 (2010) 444–450.
[20] Z. Xu, F. Cheng, C. Da, G. Liu, Y. Tang, Pharmacophore modeling of human adenosine receptor A2A antagonists, J. Mol. Model. 16 (2010) 1867–1876.
[21] X. Zhao, M. Yuan, B. Huang, H. Ji, L. Zhu, Ligand-based pharmacophore model of N-aryl and N-heteroaryl piperazine alpha 1A-adrenoceptors antagonists using GALAHAD, J. Mol. Graph. Model. 29 (2010) 126–136.
[22] I. Gantz, J. DelValle, L.D. Wang, T. Tashiro, G. Munzert, Y.J. Guo, Y. Konda, T. Yamada, Molecular basis for the interaction of histamine with the histamine H2 receptor, J. Biol. Chem. 267 (1992) 20840–20843.
[23] H. Preuss, P. Ghorai, A. Kraus, S. Dove, A. Buschauer, R. Seifert, Point mutations in the second extracellular loop of the histamine H2 receptor do not affect the species-selective activity of guanidine-type agonists, Naunyn Schmiedebergs Arch. Pharmacol. 376 (2007) 253–264.
[24] H. Weinstein, D. Chou, C.L. Johnson, S. Kang, J.P. Green, Tautomerism and the receptor action of histamine: a mechanistic model, Mol. Pharmacol. 12 (1976) 738–745.
[25] S.G. Rasmussen, H.J. Choi, D.M. Rosenbaum, T.S. Kobilka, F.S. Thian, P.C. Edwards, M. Burghammer, V.R. Ratnala, R. Sanishvili, R.F. Fischetti, G.F. Schertler, W.I. Weis, B.K. Kobilka, Crystal structure of the human beta2 adrenergic G-protein-coupled receptor, Nature 450 (2007) 383–387.
[26] T. Warne, M.J. Serrano-Vega, J.G. Baker, R. Moukhametzianov, P.C. Edwards, R. Henderson, A.G. Leslie, C.G. Tate, G.F. Schertler, Structure of a beta1-adrenergic G-protein-coupled receptor, Nature 454 (2008) 486–491.
[27] P. Scheerer, J.H. Park, P.W. Hildebrand, Y.J. Kim, N. Krauss, H.W. Choe, K.P. Hofmann, O.P. Ernst, Crystal structure of opsin in its G-protein-interacting conformation, Nature 455 (2008) 497–502.
[28] S.L. Dixon, A.M. Smondyrev, E.H. Knoll, S.N. Rao, D.E. Shaw, R.A. Friesner, PHASE: a new engine for pharmacophore perception, 3D QSAR model development, and 3D database screening: 1. Methodology and preliminary results, J. Comput. Aided. Mol. Des. 20 (2006) 647–671.
[29] H. Preuss, P. Ghorai, A. Kraus, S. Dove, A. Buschauer, R. Seifert, Mutations of Cys-17 and Ala-271 in the human histamine H2 receptor determine the species selectivity of guanidine-type agonists and increase constitutive activity, J. Pharmacol. Exp. Ther. 321 (2007) 975–982.
[30] S.X. Xie, P. Ghorai, Q.Z. Ye, A. Buschauer, R. Seifert, Probing ligand-specific histamine H1- and H2-receptor conformations with NG-acylated Imidazolylpropylguanidines, J. Pharmacol. Exp. Ther. 317 (2006) 139–146.
[31] Ligprep. Schordinger, LLC, New York, NY. (2008).
[32] G. Chang, W.C. Guida, W.C. Still, An internal coordinate monte carlo method for searching conformational space, J. Am. Chem. Soc. 111 (1989) 4379–4386.
[33] J.J. Irwin, B.K. Shoichet, ZINC—a free database of commercially available compounds for virtual screening, J. Chem. Inf. Model. 45 (2005) 177–182.
[34] M. Jacobsson, P. Liden, E. Stjernschantz, H. Bostrom, U. Norinder, Improving structure-based virtual screening by multivariate analysis of scoring data, J. Med. Chem. 46 (2003) 5781–5789.
[35] Prime. Schrodinger, LLC, New York, NY. (2008).
[36] C.H. Wu, L.S. Yeh, H. Huang, L. Arminski, J. Castro-Alvear, Y. Chen, Z. Hu, P. Kourtesis, R.S. Ledley, B.E. Suzek, C.R. Vinayaka, J. Zhang, W.C. Barker, The protein information resource, Nucl. Acids Res. 31 (2003) 345–347.
[37] J.D. Thompson, D.G. Higgins, T.J. Gibson, CLUSTAL W: improving the sensitivity of progressive multiple sequence alignment through sequence weighting, position-specific gap penalties and weight matrix choice, Nucl. Acids Res. 22 (1994) 4673–4680.
[38] Maestro. Schordinger, LLC, New York, NY. (2008).
[39] Desmond. D.E. Shaw Research, Desmond Molecular Dynamics System, New York, NY. (2008).
[40] K.J. Bowers, E. Chow, H. Xu, R.O. Dror, M.P. Eastwood, B.A. Gregersen, J.L. Klepeis, I. Kolossvary, M.A. Moraes, F.D. Sacerdoti, J.K. Salmon, Y. Shan, D.E. Shaw, Scalable algorithms for molecular dynamics simulations on commodity clusters, Proc. ACM/IEEE Conf. Supercomput. (2006).
[41] W.L. Jorgensen, D.S. Maxwell, J. Tirado-Rives, Development and testing of the OPLS all-atom force field on conformational energetics and properties of organic liquids, J. Am. Chem. Soc. 118 (1996) 11225–11236.
[42] H. Heller, M. Schaefer, K. Schulten, Molecular dynamics simulation of a bilayer of 200 lipids in the gel and in the liquid crystal phase, J. Phys. Chem. 97 (1993) 8343–8360.
[43] W.L. Jorgensen, J. Chandrasekhar, J.D. Madura, R.W. Impey, M.L. Klein, Comparison of simple potential functions for simulating liquid water, J. Chem. Phys. 79 (1983) 926–935.
[44] M.A. Lomize, A.L. Lomize, I.D. Pogozheva, H.I. Mosberg, OPM: orientations of proteins in membranes database, Bioinformatics 22 (2006) 623–625.
[45] A.L. Lomize, I.D. Pogozheva, M.A. Lomize, H.I. Mosberg, The role of hydrophobic interactions in positioning of peripheral proteins in membranes, BMC Struct. Biol. 7 (2007) 44.
[46] A.L. Lomize, I.D. Pogozheva, M.A. Lomize, H.I. Mosberg, Positioning of proteins in membranes: a computational approach, Protein Sci. 15 (2006) 1318–1333.
[47] V. Kräutler, W.F.v. Gunsteren, P.H. Hünenberger, A fast SHAKE algorithm to solve distance constraint equations for small molecules in molecular dynamics simulations, J. Computat. Chem. 22 (2001) 501–508.
[48] P. Ghorai, A. Kraus, T. Birnkammer, R. Geyer, G. Bernhardt, S. Dove, R. Seifert, S. Elz, A. Buschauer, Chiral NG-acylated hetarylpropylguanidine-type histamine H2 receptor agonists do not show significant stereoselectivity, Bioorg. Med. Chem. Lett. 20 (2010) 3173–3176.
[49] F.U. Axe, S.D. Bembenek, S. Szalma, Three-dimensional models of histamine H3 receptor antagonist complexes and their pharmacophore, J. Mol. Graph. Model. 24 (2006) 456–464.
[50] MacroModel. Schordinger, LLC, New York, NY. (2008).
[51] A.L. Morris, M.W. MacArthur, E.G. Hutchinson, J.M. Thornton, Stereochemical quality of protein structure coordinates, Proteins 12 (1992) 345–364.
[52] J.C. Eriks, H. van der Goot, H. Timmerman, New activation model for the histamine H2 receptor, explaining the activity of the different classes of histamine H2 receptor agonists, Mol. Pharmacol. 44 (1993) 886–894.
[53] P.H. Nederkoorn, J.H. van Lenthe, H. van der Goot, G.M. Donne-Op den Kelder, H. Timmerman, The agonistic binding site at the histamine H2 receptor. I. Theoretical investigations of histamine binding to an oligopeptide mimicking a part of the fifth transmembrane alpha-helix, J. Comput. Aided. Mol. Des. 10 (1996) 461–478.
[54] P.H. Nederkoorn, E.M. van Gelder, G.M. Donne-Op den Kelder, H. Timmerman, The agonistic binding site at the histamine H2 receptor. II. Theoretical investigations of histamine binding to receptor models of the seven alpha-helical transmembrane domain, J. Comput. Aided. Mol. Des 10 (1996) 479–489.
[55] S. Dove, S. Elz, R. Seifert, A. Buschauer, Structure-activity relationships of histamine H2 receptor ligands, Mini. Rev. Med. Chem. 4 (2004) 941–954.
[56] Y. Tang, W. Zhu, K. Chen, H. Jiang, New technologies in computer-aided drug design: toward target identification and new chemical entity discovery, Drug Discov. Today: Technol. 3 (2006) 307–313.
[57] P. Prathipati, A. Dixit, A.K. Saxena, Computer-aided drug design: Integration of structure-based and ligand-based approaches in drug design, Curr. Comput.-Aided Drug Des. 3 (2007) 133–148.